A study on the difference of simulated air concentrations for various chemical mechanisms and photolysis rate constants used in air quality model

Che-Kai Yeh
Graduate School of Engineering Science and Technology, National Yunlin University of Science and Technology, Taiwan

Tu-Fu Chen and Ken-Hui Chang*
Department of Safety, Health and Environmental Engineering, National Yunlin University of Science and Technology, Taiwan

1. INTRODUCTION

Ozone is a secondary pollutant and formed through a series of photochemical reactions of volatile organic compounds (VOCs) and nitrogen oxides (NOx). Ozone concentration can be predicted by air quality model and the result can be provided to support decision making or policy formulation. Consequently, the accuracy of air quality model simulation becomes significantly important. The result of air quality model is greatly affected by gaseous and aqueous phase chemical reaction, transport, deposition as well as topography and meteorological conditions. Atmospheric chemistry mechanisms play the most important role in the atmospheric chemistry model (Stockwell et al., 1997).

A number of simulation results of box model and 3-D air quality model were used to compare the differences among various chemical mechanisms (Gross and Stockwell, 2003; Jimenez et al., 2003; Chen et al., 2010; Yu et al., 2010; Ying and Li, 2011). Regional Atmospheric Chemistry Mechanism (RACM) is an atmospheric chemistry mechanism based on the Regional Acid Deposition Model, version 2 (RADM2) (Stockwell et al., 1990) and developed by Stockwell et al. (1997), which consisted of 77 chemical species and 237 reactions including photolysis that usually plays the initiative role for many chemical reactions in the atmosphere. Good photolysis rate estimates must be made to accurately predict the effects of air pollution. The photolysis rate is mainly influenced by absorption cross sections and quantum yields functioned of wavelength and temperature. The parameters of photolysis rate used in RADM2 and RACM are the data of earlier studies, thereafter many studies for photolysis rate were published and new data are available currently. What is the impact of updated photolysis rate on simulation results for various chemical mechanisms is an interesting topic for improving the performance of air quality model. Therefore, this study is subject to compare the differences of simulated ozone concentrations for RADM2, RACM mechanisms and photolysis rate constants used in Models-3/CMAQ.

*Corresponding author: Ken-Hui Chang, Department of Safety, Health and Environmental Engineering, National Yunlin University of Science and Technology, 123 university Rd. Sec. 3, Touliu, Yunlin, Taiwan. Tel.: +886 5 5342601x4417; fax: +886 5 5312069.; e-mail:changken@yuntech.edu.tw

2. Methods

Based on the RADM2 module used in Models-3/CMAQ, the gas-phase chemical mechanism is modified to establish the RACM module. In addition, the new parameters of photolysis rate are also collected to update the RADM2 and RACM modules in this study.

2.1 Establish of RACM module

Comparing to RADM2, the number of chemical reactions in RACM is significant increase. Moreover, a number of products, coefficients, reaction rates and carbon numbers need to be changed for establishing RACM module. Chemical reactions can be divided into two parts of photolysis and non-photolysis. Type of reaction, reactant, product and its coefficient are necessary to be set up in photolysis reaction. The steps for establishing the RACM module are described as follows:

2.2 Updating photolysis rate constants

There are two major data sources of absorption cross sections and quantum yields to update and adopt the photolysis rate constants in this study. One is published by Sander et al. (2006) and another is the online search system

(http://www.atmosphere.mpg.de/enid/2.html) of the atmospheric chemistry department of the Max Planck Institute (MPI). Most of the rate constants of the photolytic species can be updated in RADM2 module. A comparison of data sources of absorption cross sections and quantum yields before and after updating is listed in Table 1. The wavelength ranges have little difference after data updating, the wavelength range become greater for most part of species, but it become smaller for some species. For example, the wavelength range of NO_3 is 5 nm before updating, but shortened to 1 nm after updating. A photolytic rate constant is calculated by integrating the products of the absorption cross section and quantum yield corresponding to each wave band. Consequently, more detailed data are helpful to the accuracy of rate constant calculation.

Table 1 Comparison of data sources of absorption cross sections and quantum yields before and after updating for various species

Species	Before Updating			After Updating		
	Cross Section		Quantum Yield	Cross Section		Quantum Yield
	Wavelength rang (nm)	Reference	Reference	Wavelength range (nm)	Reference	Reference
NO_2	185 ~ 427	Base et al. (1976)	Gardner et al. (1987)	242 ~ 665	Sander et al. (2006)	Troe et al. (2000)
O_3	185 ~ 735	DeMore et al. (1988)	Moortgat et al. (1978)	185 ~ 830	Sander et al. (2006)	DeMore et al. (1994)
O_3	185 ~ 735	DeMore et al. (1988)	Stockwell et al. (1990)	185 ~ 830	Sander et al. (2006)	Stockwell et al. (1997)
HONO	310 ~ 392	Stockwell and Calvert (1978)	Stockwell et al. (1990)	184 ~ 397	Sander et al. (2006)	DeMore et al. (1994)
HNO_3	190 ~ 327	Molina and Molina (1981)	Stockwell et al. (1990)	190 ~ 352	Sander et al. (2006)	Stockwell et al. (1997)
HNO_4	188 ~ 332	Molina and Molina (1981)	Stockwell et al. (1990)	190 ~ 352	Sander et al. (2006)	Stockwell et al. (1997)
NO_3	402 ~ 695	Graham and Johnston (1978)	Magnotta et al. (1980)	403 ~ 692	Sander et al. (2006)	Johnston et al. (1996)
NO_3	402 ~ 695	Graham and Johnston (1978)	Magnotta et al. (1980)	403 ~ 692	Sander et al. (2006)	Johnston et al. (1996)
H_2O_2	190 ~ 352	Lin et al.(1978)	Stockwell et al. (1990)	190 ~ 355	Sander et al. (2006)	Stockwell et al. (1997)
HCHO	246 ~ 367	Moortgat et al. (1980, 1983)	Moortgat et al. (1983)	226 ~ 375	Sander et al. (2006)	Smith et al. (2002)
HCHO	246 ~ 367	Moortgat et al. (1980, 1983)	Moortgat et al. (1983)	226 ~ 375	Sander et al. (2006)	Moortgat et al. (1983)
ALD	206 ~ 352	Calvert and Pitts (1966)	Meyrahn et al. (1981)	202 ~ 361	Sander et al. (2006)	Atkinson et al. (1984)
OP1	210 ~ 357	Molina and Arguello (1979)	Stockwell et al. (1990)	210 ~ 370	Sander et al. (2006)	DeMore et al. (1994)
OP2	210 ~ 357	Molina and Arguello (1979)	Stockwell et al. (1990)	210 ~ 370	Sander et al. (2006)	DeMore et al. (1994)
PAA	190 ~ 352	Giguere and Olmos (1956)	Stockwell et al. (1990)	190 ~ 355	Sander et al. (2006)	Stockwell et al. (1997)
KET	277 ~ 322	Calvert and Pitts (1966)	Gardner et al. (1984)	202 ~ 355	Martinez et al.(1992)	Gardner et al. (1984)
GLY	232 ~ 457	Plum et al. (1983)	Carter et al. (1989)	232 ~ 526	Sander et al. (2006)	Atkinson et al. (1992)
GLY	232 ~ 457	Plum et al. (1983)	Carter et al. (1989)	232 ~ 526	Sander et al. (2006)	Atkinson et al. (1992)
MGLY	232 ~ 457	Plum et al. (1983)	Carter et al. (1989)	200 ~ 493	Sander et al. (2006)	Carter et al. (1989)
DCB	185 ~ 362	Carter et al. (1989)	Carter et al. (1989)	185 ~ 362	Carter et al. (1989)	Carter et al. (1989)
ONIT	263 ~ 327	Calvert and Pitts (1966)	Stockwell et al. (1990)	270 ~ 330	Atkinson et al. (1997)	Atkinson et al. (1997)
MACR	226 ~ 380	Gardner et al. (1987)	Gardner et al. (1987)	250 ~ 395	Sander et al. (2006)	Gierczak et al. (1997)
HKET	277 ~ 322	Calvert and Pitts (1966)	Gardner et al. (1984)	202 ~ 355	Martinez et al.(1992)	Gardner et al. (1984)

2.3 Air quality modeling

The meteorological conditions were generated by the MM5 with three-level nested domains as shown in Fig. 1, including East Asia in domain 1 with 81 km ×81 km resolution, southeastern China and Taiwan in domain 2 with 27 km×27 km resolution, and entire Taiwan in domain 3 with 9 km ×9 km resolution. The ozone episode of May 22 to May 29, 2003 was selected to be simulated in this study because observed data of ozone and its precursor were available.

Taiwan emission inventory dataset for 2003, called TEDS 6.03 (CTCI, 2006), was used in this study for anthropogenic emissions and Taiwan biogenic emission inventory system, called TBEIS 2.0 (Chang et al., 2009) was used to estimate biogenic emissions in Taiwan. The biogenic emission of East Asia was estimated by a model which structure is similar with TBEIS 2.0 The anthropogenic emission of East Asia majorly adopted the inventory dataset of REAS (Ohara et al., 2007) and the quantity of emission was distributed to 1km × 1km resolution based on the population distribution in East Asia with the same resolution.

Fig. 1 Modeling framework with three-level nested domains in this study

2.4 Description of simulation cases

To examine RADM2 and RACM and the influence before and after updating photolysis rates, four simulation cases were designed as Table 2. Chemical reaction mechanism RADM2 and its original photolysis rates were used in Case 1. RADM2 and the updated photolysis rates in this study were adopted in Case 2. Chemical reaction mechanism RACM and original photolysis rates of RACM were used in Case 3. RACM and the photolysis rates collected in this study were applied in Case 4.

Table 2 Chemical reaction mechanism and photolysis rate adopted in various simulation Cases

Simulation case	Chemical reaction mechanism	Photolysis rate
Case 1	RADM2	Original data in RADM2
Case 2	RADM2	Updated data in this study
Case 3	RACM	Original data in RADM2 and set up for the others in this study
Case 4	RACM	Set up in this study

3. Results and Discussion

Case 1 was served as the base case for a comparison with other cases and the influences of different change factors on model simulations were analyzed. All of the ozone concentration distribution charts below were the simulation results at 2 p.m. of May 27, 2003.

3.1 Influence of updating photolytic rate constants

The simulated ozone concentration in Case 1 was illustrated in Fig. 2a and the areas with a high ozone concentration of more than 120 ppb include Beijing, Shanghai, Korea and the southwestern coast of Taiwan. Highly ozone distributed areas in Case 2 were similar to those in Case 1; however, the areas with an ozone concentration of more than 120 ppb extended compared with Case 1. Spatial distribution differences of ozone concentrations before and after updating photolytic rate constants in domain 1 were shown in Fig. 2b. The highest increase in simulated ozone concentrations was in the coastal areas of Korea by 12 to 16 ppb, followed by Beijing, and Taiwan with an ozone increase of 4 to 8 ppb. The influence of ozone concentrations on other areas was less than 4 ppb.

3.2 Influence of various chemical reaction mechanisms

To understand the influence between RADM2 and RACM on ozone concentration, the results of Case 1 and Case 3 was compared. Spatial distribution differences of simulated ozone

concentrations between Case 1 and Case 3 in domain 1 were shown in Fig. 2c. The result of Case 3 indicated highly ozone distributed areas were similar to those in Case 1; nevertheless, areas with a high concentration expanded. The largest difference of ozone concentration is over 28 ppb and occurred along the coastal areas in Korea.

3.3 Influence of various chemical reaction mechanisms with updating photolysis rates

To analyze the effects of various chemical reaction mechanisms with updating photolysis rates, a comparison of ozone concentration between Cases 1 and 4 was made. Spatial distribution differences of ozone concentrations in domain 1 were shown in Fig. 2d. The areas that ozone concentrations were less significant like Taiwan and Guangdong in Case 1 had also increased in Case 4. Districts with the greatest concentration difference in these two cases were in Beijing, Shenyang and coastal areas in Korea. An ozone concentration difference of about 28 ppb occurred in the aforesaid districts when RADM2 was replaced by RACM with updated photolysis rates.

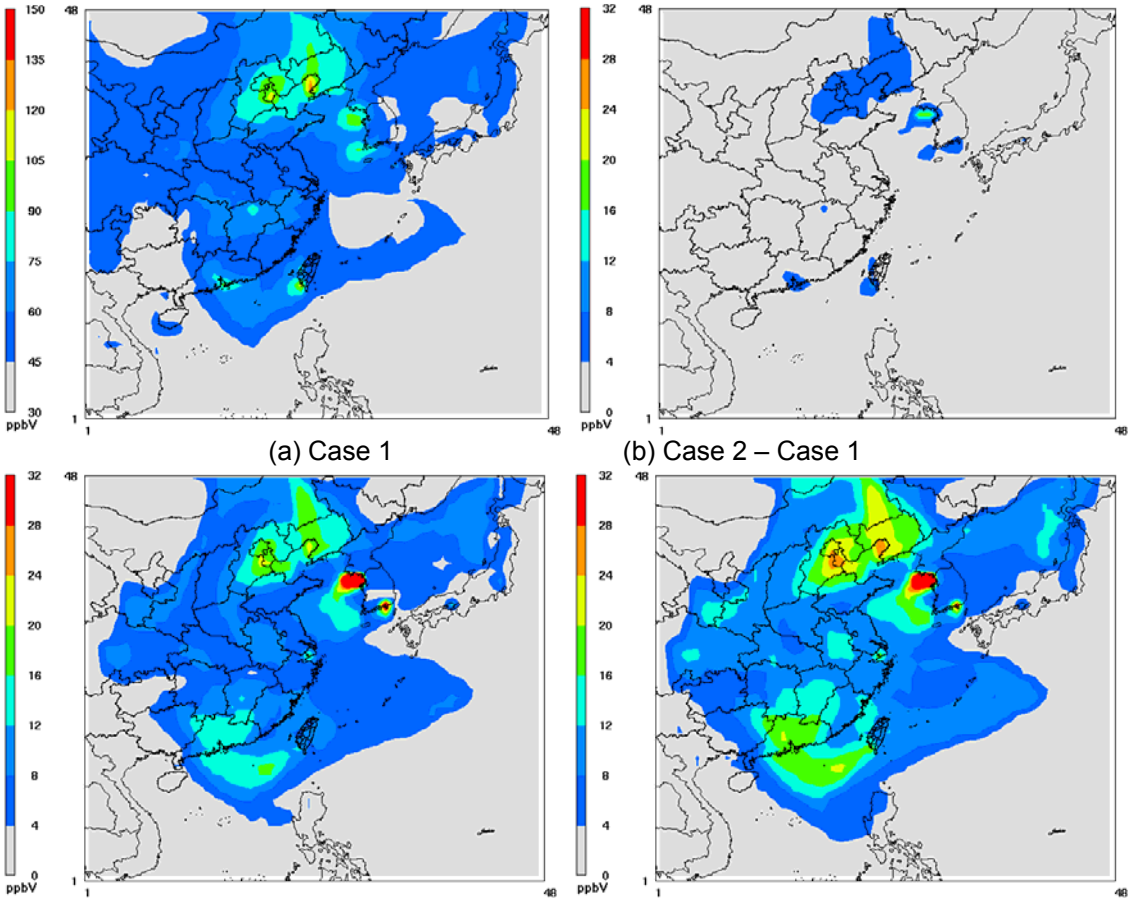

(a) Case 1 (b) Case 2 – Case 1

(c) Case 3 – Case 1 (d) Case 4 – Case 1

Fig. 2 Spatial distribution differences of ozone concentrations for various cases in domain 1

4. Conclusion

RACM module was established based on RADM2 used in CMAQ and photolysis rate constants were also updated by the new published data in this study. Four combinations of RADM2 and RACM modules with original and updated photolysis rates in CAMQ were simulated and compared to each other. According to the air quality model simulation Cases 2 thru 4 and a comparison with the simulation results of the base case, the greatest difference of the peak concentration level of ozone occurred in the southwestern Taiwan. If the photolysis rate constants were updated, the peak ozone concentration level in these areas increased by

about 12 ppb (10%). If using RACM without updating the photolytic rate constants, an increase of about 20 ppb (16%) in the peak ozone concentration level occurred in southwestern Taiwan. When RACM with updated photolysis rate constants was used, a difference in the peak ozone concentration level would be over 28 ppb (approx. 23%). The ozone concentration simulated by CMAQ with RACM mechanism was higher than those in CMAQ with RADM2.

5. References

Atkinson, R., and A. C. Lloyd, 1984: Evaluation of kinetic and mechanistic data for modeling of photochemical smog. *J. Phys. Chem.* Ref. Data 13:315-444.

Atkinson, R., D. L. Baulch, R. A. Cox, R. F. Hampson, J. A. Kerr and J. Troe, 1992: Evaluated kinetic and photochemical data for atmospheric chemistry: Supplement IV. *J. Phys. Chem*. Ref. Data, 21, 1125-1568.

Atkinson, R., D. L. Baulch, R. A. Cox, R. F. Hampson, J. A. Kerr, M. J. Rossi and J. Troe, 1997: Evaluated kinetic, photochemical and heterogeneous data for atmospheric chemistry: Supplement V. *J. Phys.Chem*. Ref. Data, 26, 521-1011.

Bass, A. M., A. E. Ledford, Jr. and A. H. Laugfer, 1976: Extinction coefficients of and N_2O_4. *J. Res. Natl. Bur. Stand.*, Sect. A, 80, 143-166.

Burrows, J. P., A. Richter, A. Dehn, B. Deters, S. Himmelmann, S. Voigt and J. Orphal, 1999: Atmospheric remote-sensing reference data from GOME: Part 2. Temperature-dependent absorption cross-sections of O_3 in the 231-794 nm range. *J. Quant. Spectrosc. Radiat. Transfer*, 61, 509-517.

Calvert, J. G. and J. N. Pitts, Jr. , 1966: Photochemistry. John Wiley, New York.

Carter, W. P. L. and R. Atkinson, 1989: Alkyl nitrate formation from the atmospheric photooxidation of alkanes: A revised estimation method. *J. Atmos. Chem.*, 8, 165-173.

Chang, K.H., Jhih-Yuan Yu, Tu-Fu Chen, Yi-Pin Lin, 2009: Estimating Taiwan biogenic VOC emission: Leaf energy balance consideration. *Atmospheric Environment*, 43, 5092-5100.

Chen, S., X. Ren, J. Mao, Z. Chen, W. H. Brune, B. Lefer, B. Rappenglück, J. Flynn, J. Olson, and J. H. Crawford, 2010: A comparison of chemical mechanisms based on TRAMP-2006 field data. *Atmospheric Environment*, 44, 4116–4125.

CTCI, 2005: *Update and Management of Air Pollution Emission Inventory and Air Pollution Degradation Estimation*. China Technological Consultant Inc., Taipei, Taiwan (in Chinese).

DeMore, W. B., S. P. Sander, M. J. Molina, D. M. Golden, R. F. Hampson, M. J. Kurylo, C. J. Howard, and A. R. Ravishankara, 1988: Chemical Kinetics and Photochemical Data for Use in Stratospheric Modeling, Evaluation Number 8, National Aeronautics and Space Administration, *Jet Propulsion Laboratory*, California Institute of Technology, Pasadena.

Gardner, E. P., R. D. Wijayaratne and J. G. Calvert, 1984: Primary quantum yields of photodecomposition of acetone in air under tropospheric conditions. *J. Phys. Chem.*, 88, 5069-5076.

Gierczak, T., J. B. Burkholder, R. K. Talukdar, A. Mellouki, S. B. Barone and A. R. Ravishankara, 1997: Atmospheric fate of methyl vinyl ketone and methacrolein. *J. Photochem. Photobiol. A: Chem.*, 110, 1-10.

Giguere, P. A. and A. W. Olmos, 1956: Sur le spectre ultraviolet de l'acide peracétique et l'hydrolyse des peracétates. *Can. J. Chem.*, 34, 689-691.

Graham, R. A. and H. S. Johnson, 1978: The photochemistry of NO_3 and the kinetics of the N2O5-O3 system. *J. Phys. Chem.*, 82, 254-268.

Gross, A., and W. R. Stockwell, 2003: Comparison of the EMEP, RADM2 and RACM Mechanisms. *Journal of Atmospheric Chemistry*, 44, 151–170.

Jimenez, P., J. M. Baldasano, D. Dabdub, 2003: Comparison of photochemical mechanisms for air quality modeling. *Atmospheric Environment*, 37, 4179–4194.

Johnston, H. S., H. F. Davis and Y. T. Lee, 1996: NO3 photolysis product channels: Quantum yields from observed thresholds. *J. Phys. Chem.*, 100, 4713-4723.

Lin, C. L., N. K. Rohatgi and W. B. DeMore, 1978: Ultraviolet absorption cross sections of hydrogen peroxide. *Geophys. Res. Lett.*, 5, 113-115.

Magnotta, F. and H. S. Johnson, 1980: Photodissociation quantum yields for the NO_3 free radical. *Geophys. Res. Lett.*, 7, 769-772.

Martinez, R. D., A. A. Buitrago, N. W. Howell, C. H. Hearn and J. A. Joens, 1992: The near UV absorption spectra of several aliphatic aldehydes and ketones. *Atmospheric Environment*, 26A, 785-792.

Meyrahn, H., G. K. Moortgat and P. Warneck, 1981: The photolysis of acetaldehyde under

atmospheric conditions. *Atmospheric Trace Constituents*, 65-72.

Middleton, P., W. R. Stockwell, W. P. Carter, 1990: Aggregation and Analysis of Volatile Organic Compound Emissions for Regional Modeling. *Atmospheric Environment*, 24A, pp.1107-1133.

Molina, L. T. and G. Arguello, Ultraviolet absorption spectrum of methylhydroperoxide vapor. *Geophys. Res. Lett.*, 6, 953-955, 1979.

Molina, L. T. and M. J. Molina, 1981: UV absorption cross sections of HO2NO2 vapor. *J. Photochem.*, 15, 97-108.

Molina, L. T. and M. J. Molina, 1986: Absolute absorption cross sections of ozone in the 185- to 350-nm wavelength range. *J. Geophys. Res.*, 91, 14501-14508.

Moortgat, G. K. and E. Kudzus, 1978: Mathematical expression for the O(1D) quantum yields from O3 photolysis as a function of temperature (230-320 K) and wavelength (298-320 nm). *Geophys. Res. Lett.*, 5, 191-194.

Moortgat, G. K., W. Klippel, K. H. Mobus, W. Seiler and P. Wameck, 1980: Laboratory measurement of photolytic parameters for formaldehtde, Final Rep. FAA-EE-80-47, Office of Environ. And Encrgy, Fed Aviat. Admin., Washington, D. C..

Moortgat, G. K., W. Seiler and P. Warneck, 1983: Photodissociation of HCHO in air: CO and H2 quantum yields at 220 and 330 K. *J. Chem. Phys.*, 78, 1185-1190.

Plum, C. N., E. Sanhueza, R. Atkinson, W. P. L. Carter and J. N. Pitts, Jr. , 1983: OH radical rate constants and photolysis rates of α dicarbonyls. *Environ. Sci. Technol.*, 17, 479-489.

Sander, S.P., R. R. Friedl, A. R. Ravishankara, D. M. Golden, C. E. Kolb, M. J. Kurylo, M. J. Molina, G. K. Moortgat, B.J. Finlayson-Pitts, P. H. Wine, R. E. Huie, V. L. Orkin, 2006: Chemical Kinetics and Photochemical Data for Use in Atmospheric Studies. Evaluation Number 15, JPL Publication 06-02, Jet Propulsion Laboratory, Pasadena, California.

Smith, G. D., L. T. Molina and M. J. Molina, 2002: Measurement of Radical Quantum Yields from Formaldehyde Photolysis between 269 and 339 nm. *J. Phys. Chem. A*, 106, 1233-1240.

Stockwell. W. R. and J. G. Calvert, 1978: The near ultraviolet spectrum of gaseous HONO and N2O3. *J. Photochem.*, 8, 193-203.

Stockwell, W. R., P. Middleton, J. S. Chang, X. Tang, 1990: The second generation regional Acid Deposition Model chemical mechanism for regional air quality modeling. *J. Geophys. Res.*, 95, 16343-16367.

Stockwell, W. R., F. Kirchner, M. Kuhn, S. Seefeld, 1997: A new mechanism for regional atmospheric chemistry modeling. *J. Geophys. Res.*, 102, 25847-25880.

Troe, J., Z., 2000: Are primary quantum yields of NO2 photolysis at λ ≤ 398 nm smaller than unity? *Phys. Chem.*, 214, 573-581.

Ying Q. and J. Li, 2011: Implementation and initial application of the near-explicit Master Chemical Mechanism in the 3D Community Multiscale Air Quality (CMAQ) model. *Atmospheric Environment*, 45, 3244-3256.

Yu, S., R. Mathur, G. Sarwar, D. Kang, D. Tong, G. Pouliot, and J. Pleim, 2010: Eta-CMAQ air quality forecasts for O3 and related species using three different photochemical mechanisms (CB4, CB05, SAPRC-99): comparisons with measurements during the 2004 ICARTT study. *Atmos. Chem. Phys.*, 10, 3001–3025.